



Cite this: DOI: 10.1039/c6md00440g

An unexpected reversal in the pharmacological stereoselectivity of benzothiadiazine AMPA positive allosteric modulators†‡

 Umberto M. Battisti,^{§ab} Cinzia Citti,^{§cd} Giulio Rastelli,^a Luca Pinzi,^a Giulia Puja,^a Federica Ravazzini,^a Giuseppe Ciccarella,^{cd} Daniela Braghioroli^a and Giuseppe Cannazza^{*ad}

Benzothiadiazine type compounds (BTDs) have gained great attention for their potential therapeutic activity as nootropic and neuroprotective agents. BTDs, acting as AMPA positive allosteric modulators, potentiate the glutamatergic neurotransmission without the side effects typically associated with direct agonists. Studies regarding the binding mode of racemic BTDs into the receptor binding pocket demonstrated that one enantiomer establishes a more favourable interaction and possesses a higher biological activity with respect to the other one. The *S* enantiomer was proved to be the eutomer for both IDRA21 and S18986, two of the most studied BTD AMPA positive allosteric modulators. However, recent data highlighted an opposite stereoselectivity for some substituted BTDs (7-chloro-9-(furan-3-yl)-2,3,3a,4-tetrahydro-1*H*-benzo[e]pyrrolo[2,1-*c*][1,2,4]thiadiazine 5,5-dioxide and 7-chloro-2,3,4-trimethyl-3,4-dihydro-2*H*-benzo[e]-[1,2,4]thiadiazine 1,1-dioxide) showing unexpected structure–activity relationships. In this work, the synthesis and configuration assignment of the stereoisomers of 7-chloro-5-(3-furanyl)-3-methyl-3,4-dihydro-2*H*-1,2,4-benzothiadiazine 1,1-dioxide, one of the most active BTDs, are reported. Electrophysiological tests demonstrated that the *R* form is the eutomer. Docking and molecular dynamics simulations on the AMPA GluA2 binding site revealed new insights into the stereodiscrimination process. Lastly, metabolic studies disclosed a stereoselective hepatic metabolization of this chiral BTD.

 Received 1st August 2016,
Accepted 26th September 2016

DOI: 10.1039/c6md00440g

www.rsc.org/medchemcomm

1. Introduction

L-Glutamate is the major excitatory neurotransmitter in the mammalian central nervous system (CNS) activating metabotropic glutamate receptors (coupled to G proteins) and ionotropic glutamate receptors (iGluRs).^{1–3} On the basis of their sensitivity to selective agonists, iGluRs have been further classified into three subclasses: kainic acid (KA), *N*-methyl-D-aspartic acid (NMDA) and α -amino-3-hydroxy-5-methyl-4-isoxazolepropionic acid (AMPA) receptors.^{1–3} Among

these three subclasses, AMPA receptors (AMPA receptors) modulate fast excitatory postsynaptic signaling and are involved in long-term potentiation, a process related to learning and memory establishment.^{4,5} For these reasons, AMPARs represent an interesting target for the development of cognitive enhancers. In fact, there is rapidly growing interest in AMPA positive allosteric modulators (AMPA PAMs) as potentiators of the glutamatergic function.⁶ Compared to direct AMPA receptor agonists, allosteric modulators are anticipated to possess finer tuning to increase glutamatergic function since they have no effects in the absence of the natural ligand in the synapse. Different studies highlighted a possible role for AMPA PAMs in the therapeutic strategy to treat central nervous system (CNS) disorders,⁷ such as schizophrenia,⁸ Alzheimer's disease,⁹ attention-deficit/hyperactivity disorder (ADHD),¹⁰ and depression.¹¹

Several chemical classes of AMPA PAMs have been described in the past years; among them, benzothiadiazines (BTD) represent one of the most investigated classes.^{6,12} Classical examples of BTD modulators are cyclothiazide (1, Fig. 1), IDRA21 (2, Fig. 1) and S18986 (S-3, Fig. 1). Cyclothiazide was one of the first reported BTDs active as AMPA PAM, and it is still widely used as a pharmacological tool.

^a Department of Life Sciences, University of Modena & Reggio Emilia, Via Campi 103, 41125 Modena, Italy. E-mail: giuseppe.cannazza@unimore.it; Fax: +39 059 2055131; Tel: +39 059 2058575

^b Department of Medicinal Chemistry, School of Pharmacy, Virginia Commonwealth University, Richmond, Virginia 23298, USA

^c Department of Biological and Environmental Sciences and Technologies, University of Salento, Via per Monteroni, 73100 Lecce, Italy

^d CNR-NANOTEC, Campus Ecotekne of the University of Salento, Via per Monteroni, 73100 Lecce, Italy

† The authors declare no competing interests.

‡ We dedicate this work to Professor Carlo Parenti on the occasion of his retirement, who, with his great experience and dedication to organic synthesis, has given important contributions to scientific research.

§ These authors contributed equally to this work.

IDRA21 has attracted particular clinical interest despite its poor *in vitro* activity since it is effective in increasing learning and memory performances in behavioural tests, representing an important lead compound able to cross the blood–brain barrier (BBB). Compound S-3, from Servier, is the only BTD clinically evaluated as an AMPA PAM.

Recent crystallographic studies regarding the binding mode of BTD derivatives on S1S2 GluA2 subunits of AMPAR suggested that these compounds bind to the dimer interface, leading to inhibition of the receptor desensitization by stabilization of the ligand-binding domain within a dimer interface.¹³ In particular, a detailed analysis of the crystal structures of IDRA21 and cyclothiazide in complex with S1S2 GluA2 subunits revealed that, notwithstanding they share the same 1,2,4-benzothiadiazine 1,1-dioxide scaffold, different substituents in the 3-position of the thiadiazine ring lead to a shifted binding mode of 2 compared to that of 1.¹⁴

By exploiting these crystallographic data, we designed and synthesized 7-chloro-5-(3-furanyl)-3-methyl-3,4-dihydro-2H-1,2,4-benzothiadiazine 1,1-dioxide (4, Fig. 1); this molecule exhibited an interesting pharmacological activity as AMPA PAM as well as good BBB permeability.¹⁵ Recently, we synthesized the single stereoisomers of 7-chloro-9-(furan-3-yl)-2,3,3a,4-tetrahydro-1H-benzo[e]pyrrolo[2,1-c][1,2,4]-thiadiazine 5,5-dioxide.¹⁶ The latter was designed as a chimeric compound between 3 and 4. Among the two stereoisomers, (R)-7-chloro-9-(furan-3-yl)-2,3,3a,4-tetrahydro-1H-benzo[e]pyrrolo[2,1-c][1,2,4]thiadiazine 5,5-dioxide (R-5, Fig. 1) proved to be the eutomer. A similar finding was reported by Larsen *et al.* for (R)-7-chloro-2,3,4-trimethyl-3,4-dihydro-2H-benzo[e][1,2,4]thiadiazine 1,1-dioxide (BPAM-321, R-6, Fig. 1).¹⁷

The crystallographic data proved unambiguously that the R enantiomer is the bioactive species of the latter compound. Both findings are in complete disagreement with all the evidence and data gathered for IDRA21 and S18986, their respective lead compounds, for which the active enantiomer is reported to be the S form.^{14,18} These new findings give rise to

the problem of having reliable structure–activity relationships as well as a consistent binding mode prediction for BTD compounds in the S1S2 GluA2 ligand binding site. In this work, we reported the synthesis of the stereoisomers of 4 and their configuration assignment and biological activity in order to unambiguously identify the bioactive form. Docking and molecular dynamics simulations were then employed to rationalize the biological results. Finally, the hepatic stereoselective metabolism of compound 4 was evaluated by using a chiral LC-MS/MS method.

2. Results and discussion

2.1 Chemistry

The synthetic pathway employed is shown in Scheme 1.¹⁵ Halogenation of 2-amino-5-chlorobenzenesulfonamide (7) under acidic conditions gave 8, which subsequently afforded intermediate 9 by Pd-catalyzed cross-coupling reaction with 3-furanylboronic acid. Racemic 4 was finally obtained by ring closure with acetaldehyde under catalytic acidic conditions. The single enantiomers of compound 4 were then obtained by chiral semipreparative HPLC.

Since previous studies on benzothiadiazines structurally similar to 4 suggested that protic solvents could trigger a racemization process, the enantioseparation of 4 was performed on ChiraSpher® NT column employing *n*-hexane/THF 75:25 (v/v) as an eluent (Fig. 2).¹⁹ The enantiomeric excess was evaluated by a chiral LC-MS/MS protocol, as described in the methods section, using an analytical Chiralcel® OD-RH. The first and second eluted isomers showed an enantiomeric excess of 96% and 97%, respectively.

The first eluted enantiomer gave an $[\alpha]_D$ of +134.0 (2 mg mL⁻¹, acetone, *T* = 24 °C), whereas the second eluted enantiomer gave an $[\alpha]_D$ of -140.0 (2.2 mg mL⁻¹, acetone, *T* = 24 °C). The difference between the two optical rotations was probably due to the slightly different enantiomeric excess. Both circular dichroism (CD) and UV spectra of the two enantiomers were acquired (Fig. 3). Whilst the two UV spectra perfectly overlapped, the CD spectra of the two enantiomers showed an opposite cotton effect. The comparison between the CD spectra of the two enantiomers and the CD spectra of enantiomers of other BTD type compounds similar to 4 allowed for the assignment of the absolute configuration of the enantiomers under investigation: the S configuration was assigned to the dextrorotatory isomer and the R configuration to the levorotatory one.

2.2 Biological activity

The activity of compound 4 and its enantiomers as allosteric modulators of AMPA/kainate receptors was evaluated by the patch-clamp technique in primary cultures of cerebellar neurons. Kainate (KA)-evoked currents were mainly mediated by AMPAR activation because application of GYKI 53655 (100 μM), an AMPAR antagonist, almost completely abolished the currents (data not shown). Since IDRA21 is one of the most

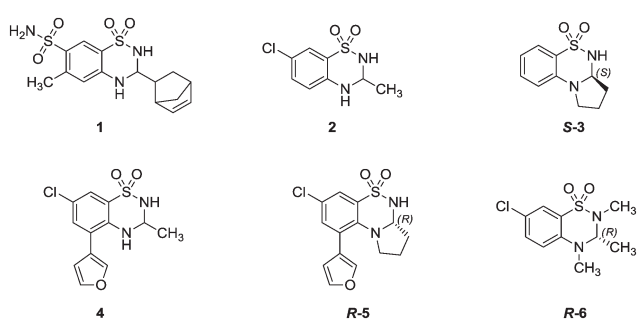
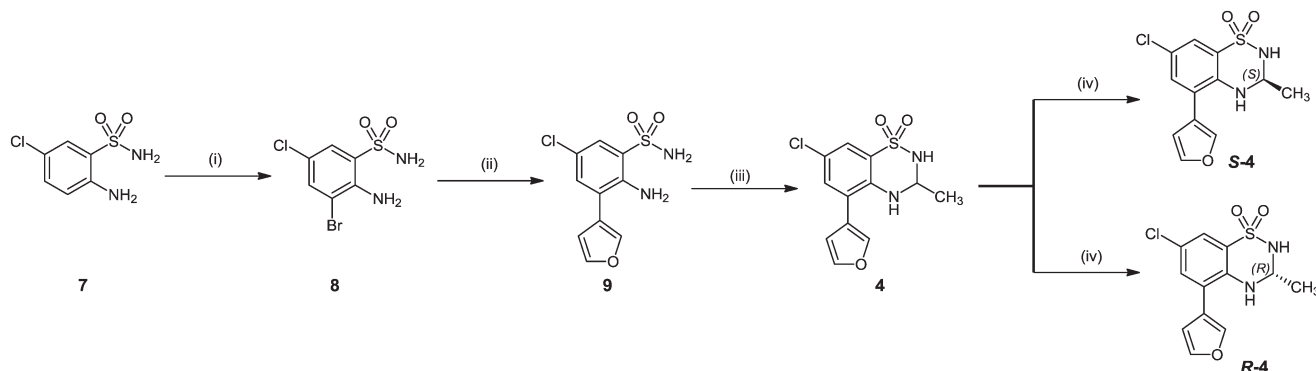


Fig. 1 Chemical structures of BTD AMPA PAMs: cyclothiazide (1), IDRA 21 (2), S18986 (S-3) 7-chloro-5-(3-furanyl)-3-methyl-3,4-dihydro-2H-1,2,4-benzothiadiazine 1,1-dioxide (4), (R)-7-chloro-9-(furan-3-yl)-2,3,3a,4-tetrahydro-1H-benzo[e]pyrrolo[2,1-c][1,2,4]thiadiazine 5,5-dioxide (R-5), (R)-7-chloro-2,3,4-trimethyl-3,4-dihydro-2H-benzo[e]-[1,2,4]thiadiazine 1,1-dioxide (R-6).



Scheme 1 Reagents and conditions: (i) Br_2 , AcOH, ACN; (ii) Na_2CO_3 , 3-furanylboronic acid, tetrakis(triphenylphosphine)palladium(0), H_2O /dioxane, 110°C ; (iii) CH_3CHO , HCl, *i*PrOH; (iv) ChiraSpher® NT column (250×10 mm I.D., $5 \mu\text{m}$), $200 \mu\text{L}$ loop, flow rate: 5 mL min^{-1} , mobile phase: *n*-hexane/THF (75:25, v/v). Concentration of 4: $10 \mu\text{M}$.

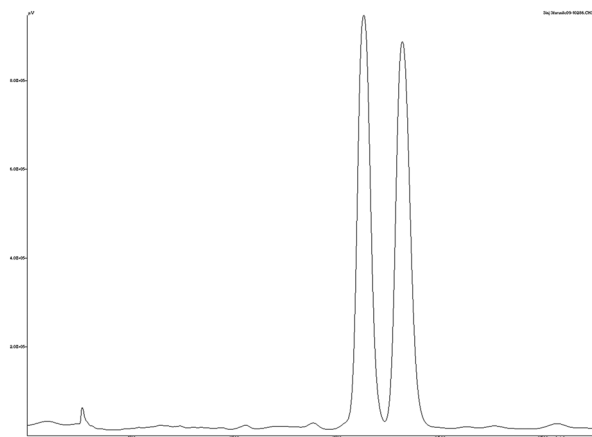


Fig. 2 Semipreparative enantioseparation of 4. Column: ChiraSpher® NT (250×10 mm I.D., $5 \mu\text{m}$), $200 \mu\text{L}$ loop, mobile phase: *n*-hexane:THF (75:25, v/v), flow rate: 5 mL min^{-1} , $\lambda_{\text{max}} = 254 \text{ nm}$, room temperature.

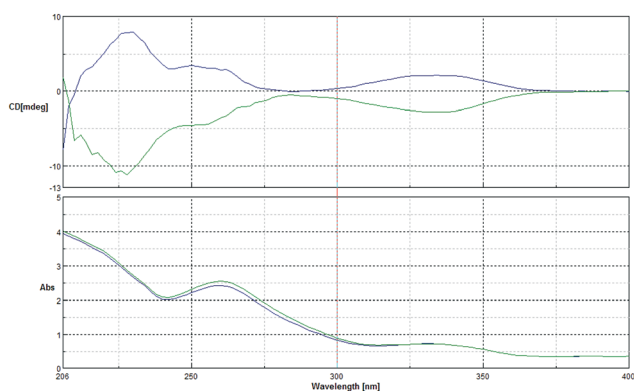


Fig. 3 Experimental CD (top) and UV (bottom) spectra of the single enantiomers of 4 obtained by semipreparative chiral chromatography. Concentration: 0.1 mg mL^{-1} in acetone:methanol (1:20, v/v); cell length: 1 mm (green line, S-4; blue line, R-4).

relevant BTD derivatives reported in the literature as AMPA PAM, it was selected as a reference compound. The data

obtained indicated that compound 4 and IDRA21 potentiated by $1603 \pm 512\%$ ($n = 4$) and $8 \pm 11\%$ ($n = 4$) the KA-evoked currents at $10 \mu\text{M}$, respectively (Fig. 4). In order to highlight possible stereospecific interactions of 4 with AMPA/kainate receptors, R-4 and S-4 were also tested. The data obtained indicated a marked difference in activity: R-4 enhanced the currents by $2586 \pm 682\%$ while S-4 by $488 \pm 370\%$. These surprising results indicated that R-4 is almost five times more active than S-4 confirming a stereospecific interaction with the receptor.

Recently, our research group has demonstrated that compound 4 is configurationally unstable in protic aqueous solvents, such as physiological solution. Anyway, the racemization rate of compound 4 is much lower than those of other benzothiadiazine type compounds ($t_{1/2} = 60 \text{ min}$ at pH 7.4 and 37°C).¹⁹

2.3 Modeling

A possible explanation of the enantiomeric preference showed by compound 4 was sought by modeling the R and S enantiomers of this compound into the AMPA allosteric binding site. To this end, the R and S enantiomers of 4 were docked into two crystal structures of the AMPAR, one in

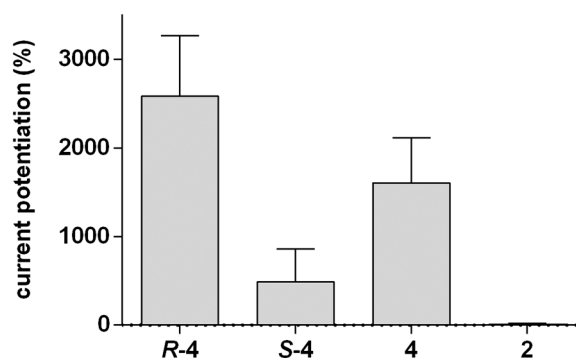


Fig. 4 Biological activity of the selected compounds. Potentiation of R-4, S-4, 4 and 2 on KA-evoked currents ($10 \mu\text{M}$). Each data point is the mean \pm SEM of at least five cells.

complex with an analogue of **4** with *S* stereochemistry (compound IDRA21, PDB code 3IL1) and the other with *R* stereochemistry (compound BPAM-321, PDB code 5BUU).^{14,17} Docking into the two crystal structures provided almost identical results (RMSD between ligand poses obtained in the two crystal structures being less than 0.8 Å). Moreover, both enantiomers of compound **4** displayed a binding mode very similar to those of IDRA21 and BPAM-321 in the corresponding 3IL1 and 5BUU crystal structures, RMSD of the common skeleton atoms being less than 0.6 Å.

Fig. 5A and B show the binding modes of *R*-**4** and *S*-**4** predicted by docking in the 3IL1 crystal structure. Both enantiomers established a network of interactions analogous to those of IDRA21 in the 3IL1 crystal structure. Moreover, sequential docking into the two adjacent allosteric pockets provided almost identical ligand poses, in agreement with available crystal structures. In both enantiomers, one sulfonamide oxygen hydrogen bonded with the Gly731 backbone amino group. A further hydrogen bond with the Pro494 carbonyl was observed only for *S*-**4**. Interestingly, superimposition of the *R*-**4** and *S*-**4** binding modes (Fig. 5C) showed that the two enantiomers adopt a very similar orientation. However, while the 2-NH group of the *S* enantiomer hydrogen bonds with the backbone carbonyl of Pro494, it is solvent exposed in the *R* enantiomer. The docking scores could not discriminate the different binding ability of the two enantiomers.

Therefore, molecular dynamics (MD) simulations in explicit solvent followed by binding free energy predictions made with MM-PBSA³¹ were performed starting from the docking complexes of *R*-**4** and *S*-**4** described above. MD simulations on both stereoisomers of IDRA21 (**2**), which showed preference for the *S* enantiomer in the crystal structure, were

also run as a control. In the resulting MD trajectories, the orientation of the two ligands in the binding pocket was maintained throughout the simulation, the average RMSD values with respect to the initial docking pose being always less than 1.3 Å. The average hydrogen bond distances between the 2-NH groups of compounds *S*-**4** and *S*-**2** and the Pro494 carbonyl were 2.1 ± 0.4 Å, while no hydrogen bond could be observed for the *R* enantiomers. Rather, in the latter stereochemistry, the 2-NH group was engaged in a hydrogen bond with a water molecule.

Binding free energy predictions are reported in Table 1. Free energies of binding (ΔG_{bind}) were calculated as the sum of the molecular mechanics contribution of the internal, electrostatic, and van der Waals contribution to binding *in vacuo* (ΔG_{vacuo}) and the solvation free energy contribution to binding expressed as the sum of polar and nonpolar solvation free energies (ΔG_{solv}). Comparison of calculated free energies of binding suggested that the *R* stereoisomer of compounds **4** and **2** binds $6.6 \text{ kcal mol}^{-1}$ more favorably and $2.5 \text{ kcal mol}^{-1}$ less favorably with respect to the corresponding *S* stereoisomer (Table 1). These data are in agreement with the inversion of the eutomer preferences for compounds **2** and **4** observed experimentally. Interestingly, interaction energies *in vacuo* were in favor of the *R* stereoisomer for compound **4** (ΔG_{vacuo} of $-2.2 \text{ kcal mol}^{-1}$) but not for compound **2**, which favored the *S* stereoisomer by $5.6 \text{ kcal mol}^{-1}$. Solvation free energies (ΔG_{solv}) were always in favor of the *R* stereochemistry, likely because in this stereochemistry the 2-NH is solvent exposed and does not hydrogen bond to the proline, thus it requires less energy to desolvate. In the case of compound **4** both energy terms cooperated to favor the *R* enantiomer, thus explaining the overall effect. This interaction with Pro494 was proved to be non-essential for the binding and the activity of BTD compounds.^{17,32} However, the data here presented and the crystallographic structure reported by Larsen *et al.* show that this residue plays a relevant role in stereodiscrimination. In fact, compounds able to form additional van der Waals interactions (e.g. **4** vs. **2**, or *R*-**6** vs. *S*-**3**) seem to prefer the *R* stereoisomer that can probably fit better into the receptor cavity. The loss of the polar interaction with Pro494, related to the *R* configuration, appears to be overcome by van der Waals interactions and/or polar interactions with water molecules.

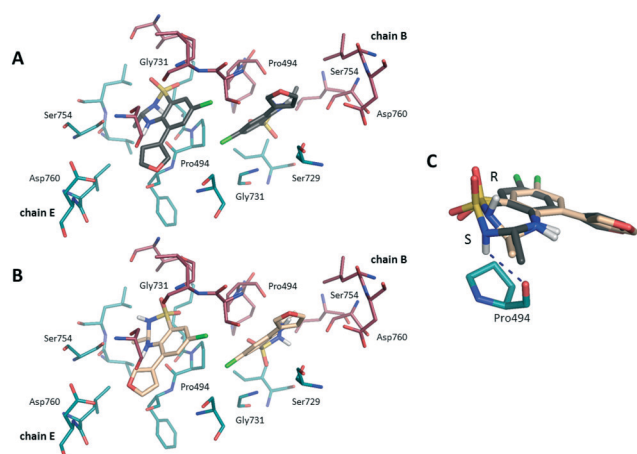


Fig. 5 Binding mode of compounds *S*-**4** (A) and *R*-**4** (B) predicted by docking in the 3IL1 crystal structure. Panel C shows a superimposition of the *S*-**4** and *R*-**4** binding modes, highlighting that the hydrogen bond with the Pro494 backbone carbonyl is possible only for *S*-**4**. The *S*-**4** and *R*-**4** enantiomers are colored in black and wheat, respectively. The two monomers (chain B and chain E) are colored in red and green, respectively. The image is created using PyMol (The PyMOL Molecular Graphics System, Version 1.8, Schrödinger, LLC).

Table 1 Binding free energy predictions (kcal mol^{-1}) made with MM-PBSA for compounds **4** and **2** in the *S* and *R* stereochemistry. For each free energy component, energy differences are always relative to those of the *S* enantiomer. ΔG_{bind} is calculated as $\Delta G_{\text{vacuo}} + \Delta G_{\text{solv}}$

	<i>S</i> - 4	<i>R</i> - 4	<i>S</i> - 2	<i>R</i> - 2
ΔG_{vacuo}	0	-2.2	0	5.6
ΔG_{solv}	0	-4.4	0	-3.1
ΔG_{bind}	0	-6.6	0	2.5

2.4 Stereoselective hepatic metabolism of 7-chloro-5-(3-furanyl)-3-methyl-3,4-dihydro-2H-1,2,4-benzothiadiazine 1,1-dioxide (4)

A simple procedure to evaluate LTD metabolism using rat liver microsomes, a subcellular fraction containing major drug-metabolizing enzymes, including the cytochrome P450 (CYP450) family and flavin monooxygenase has been recently reported.^{29,30} This protocol was successfully applied to racemic 4 indicating a fast metabolism to its unsaturated derivative 7-chloro-5-(furan-3-yl)-3-methyl-4H-benzo[*e*][1,2,4]-thiadiazine 1,1-dioxide, which demonstrated to retain most of the activity of the parent compound 4.³⁰ However, since it was possible to isolate and assign the configuration of the stereoisomers and given the difference observed in the biological activity, it is of great importance to develop a chiral version of the metabolism protocol in order to assess a possible stereoselective metabolism. Briefly, 5 μL of a 10 μM solution of racemic compound 4 was incubated with 432 μL of 0.1 M phosphate buffer, pH 7.4, 50 μL of 10 mM NADPH, and 13 μL of rat liver microsomes at a protein concentration of 20 mg mL^{-1} in the same phosphate buffer. The incubation at 37 $^{\circ}\text{C}$ was carried out at t_0 (stopped right after the addition of microsomes with ice-cold methanol) and t_{60} (stopped 60 min after the addition of microsomes). The two media (at t_0 and t_{60}) were analyzed by the same LC-MS/MS method used for the determination of the enantiomeric excess of *S*-4 and *R*-4 after semipreparative enantioseparation. The area of the peak corresponding to the *R* enantiomer was higher than that of the *S* enantiomer by about 50% after 60 minutes of incubation with the microsomes (Fig. 6). The loss (%) of the parent compound was obtained by the ratio of the

area of the peaks obtained by the LC-MS/MS injection of the sample at t_0 and that of the sample at t_{60} . The loss was about 33% for the *R* enantiomer and 62% for the *S* enantiomer. This result suggested that enantiomer *R*-4 is scarcely metabolized to the unsaturated derivative by hepatic CYP450 compared to *S*-4. In the light of the results obtained from the biological tests, these findings assume great relevance considering that a large amount of the bioactive enantiomer could reach the CNS to exert its function. To the best of our knowledge, this is the first time that a stereoselective metabolism for LTD compounds has been reported. Moreover, recent cerebral microdialysis studies carried out by our research group have highlighted that when racemic 4 was administered *in vivo* the concentration of the *R* enantiomer in the CNS was slightly higher than that of the *S* enantiomer.³² This is most likely due to the stereoselective hepatic metabolism suggested by the results reported herein.

3. Experimental

3.1 Chemicals and reagents

All chemicals and reagents, except those specifically noted, were purchased from Sigma-Aldrich (Milan, Italy). LC/MS grade water and acetonitrile (ACN) were also purchased from Sigma-Aldrich (Milan, Italy).

3.2 Chemistry

2-Amino-5-chloro-3-(3-furanyl)benzenesulfonamide (8). Compound 9 was obtained as described by Battisti *et al.*¹⁵ Yield: 70%, (28 mg, two steps), m.p.: 81–83 $^{\circ}\text{C}$. $^1\text{H NMR}$ (400 MHz, CDCl_3): δ = 5.10 (s, broad, 2H), 5.12 (s, broad, 2H), 6.56 (s, 1H), 7.32 (d, J = 2.5 Hz, 1H), 7.57 (t, J = 1.5 Hz, 1.6 Hz, 1H), 7.63 (s, 1H), 7.75 (d, J = 2.5 Hz, 1H). GC-MS (70 eV): m/z 272 (84) [M^+], 191 (67), 163 (60), 128 (100), 101 (30).

(\pm)-7-Chloro-5-(3-furanyl)-3-methyl-3,4-dihydro-2H-1,2,4-benzothiadiazine 1,1-dioxide (4). Compound 4 was obtained from compound 9 as described by Battisti *et al.*¹⁵ Yield: 99% (30 mg, one step), m.p.: 183–185 $^{\circ}\text{C}$. $^1\text{H NMR}$ (400 MHz, CDCl_3): δ = 1.54 (d, J = 6.1 Hz, 3H), 4.65 (s, 1H, broad), 4.69 (s, 1H), 5.02–5.04 (m, 1H), 6.55 (s, 1H), 7.25 (d, J = 2.5 Hz, 1H), 7.53 (d, J = 2.5 Hz, 1H), 7.58 (t, J = 1.5 Hz, 1H), 7.63 (s, 1H). GC-MS (70 eV): m/z 298 (100) [M^+], 283 (57), 192 (98), 163 (55), 128 (77), 101 (35).

***R*-(–)-7-Chloro-5-(3-furanyl)-3-methyl-3,4-dihydro-2H-1,2,4-benzothiadiazine 1,1-dioxide (*R*-4).** Compound *R*-4 was obtained by semipreparative chiral chromatography from 4 (conditions: ChiraSpher® NT column (250 \times 10 mm I.D., 5 μm ; Merck, Darmstadt, Germany), 200 μL loop, flow rate: 5 mL min^{-1} , mobile phase: *n*-hexane/THF (75 : 25, v/v), temperature: 25 $^{\circ}\text{C}$).

Yield: 81% (4 mg, 97% *ee*), m.p.: 183–185 $^{\circ}\text{C}$. $^1\text{H NMR}$ (400 MHz, CDCl_3): δ = 1.54 (d, J = 6.1 Hz, 3H), 4.65 (s, 1H, broad), 4.69 (s, 1H), 5.02–5.04 (m, 1H), 6.55 (s, 1H), 7.25 (d, J = 2.5 Hz, 1H), 7.53 (d, J = 2.5 Hz, 1H), 7.58 (t, J = 1.5 Hz, 1H),

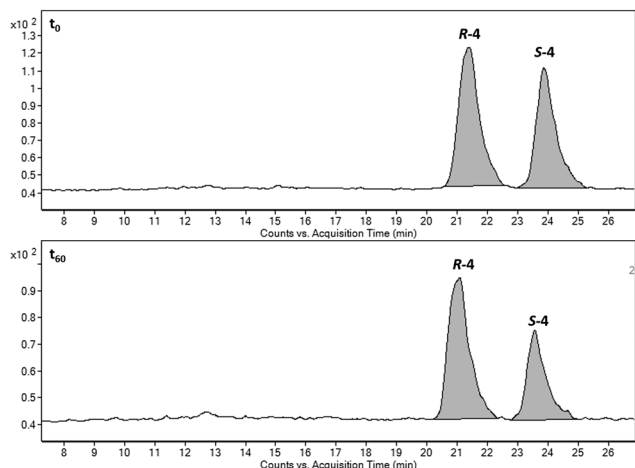


Fig. 6 MS chromatograms (positive ionization mode, SRM: 299 \rightarrow 218) of the microsomal extracts after incubation of racemic 4 with the microsomal enzymes at t_0 (top) and t_{60} (bottom). Chromatographic conditions: Chiralcel® OD-RH column (150 \times 4.6 mm I.D., 5 μm); mobile phase: water (0.1% formic acid):ACN (50:50, v/v); flow rate: 0.5 mL min^{-1} . The decrease in the peak area was about 62% for *S*-4 and about 33% for *R*-4, indicating a stereoselective metabolism of 4 by hepatic CYP450.

7.63 (s, 1H). GC-MS (70 eV): m/z 298 (100) [M^+], 283 (57), 192 (98), 163 (55), 128 (77), 101 (35). $[\alpha]_D = -140.0$ (2.2 mg mL⁻¹; acetone; 24 °C).

S-(+)-7-Chloro-5-(3-furanyl)-3-methyl-3,4-dihydro-2H-1,2,4-benzothiadiazine 1,1-dioxide (S-4). Compound S-4 was obtained by semipreparative chiral chromatography from 4 (conditions: ChiraSpher® NT column (250 × 10 mm I.D., 5 μm; Merck, Darmstadt, Germany), 200 μL loop, flow rate: 5 mL min⁻¹, mobile phase: *n*-hexane/THF (75 : 25, v/v), temperature: 25 °C).

Yield: 72% (3.6 mg, 96% *ee*), m.p.: 183–185 °C. ¹H NMR (400 MHz, CDCl₃): δ = 1.54 (d, *J* = 6.1 Hz, 3H), 4.65 (s, 1H, broad), 4.69 (s, 1H), 5.02–5.04 (m, 1H), 6.55 (s, 1H), 7.25 (d, *J* = 2.5 Hz, 1H), 7.53 (d, *J* = 2.5 Hz, 1H), 7.58 (t, *J* = 1.5 Hz, 1H), 7.63 (s, 1H). GC-MS (70 eV): m/z 298 (100) [M^+], 283 (57), 192 (98), 163 (55), 128 (77), 101 (35). $[\alpha]_D = +134.0$ (2 mg mL⁻¹; acetone; 24 °C).

3.3 Electrophysiological tests

Primary cultures of cerebellar granule neurons were prepared from 7 day old Sprague–Dawley rats as reported in the literature.²⁰ Briefly, cells from the cerebellum were dispersed with trypsin (0.24 mg mL⁻¹; Sigma Aldrich, Milan, Italy) and plated at a density of 0.8×10^6 cells per mL on 35 mm Falcon dishes coated with poly-L-lysine (10 μg mL⁻¹, Sigma Aldrich). Cells were plated in basal Eagle's Medium (BME; Celbio, Milan, Italy), supplemented with 10% fetal bovine serum (Celbio), 2 mM glutamine, 25 mM KCl and 100 μg mL⁻¹ gentamycin (Sigma Aldrich) and maintained at 37 °C in 5% CO₂. After 24 h *in vitro*, the medium was replaced with a 1 : 1 mixture of BME and Neurobasal medium (Celbio, Milan) containing 2% B27 supplement, 1% antibiotic, and 0.25% glutamine (Invitrogen). At 5 days *in vitro* (DIV5), cytosine arabinofuranoside (Ara-C) was added at a final concentration of 1 μM. Recordings were performed at room temperature, under voltage-clamp in the whole-cell configuration of the patch-clamp technique on cells. Electrodes were pulled from borosilicate glass (Heidelberg, FRG) using a vertical puller (PB-7, Narishige) and had a resistance of 5–6 MOhm. Currents were amplified using an Axopatch 1D amplifier (Axon Instruments, Foster). The recording chamber was continuously perfused at 5 mL min⁻¹ with an artificial extracellular solution composed of (mM): 145 NaCl, 5 KCl, 1 CaCl₂, 5 Hepes, 5 glucose, 20 sucrose, pH 7.4 with NaOH. The electrode intracellular solution contained (mM): 140 KCl, 3 MgCl₂, 5 EGTA, 5 Hepes, 2 ATP-Na, pH 7.3 with KOH. Drugs were applied directly by gravity using a Y-tube perfusion system.

3.4 Modeling

Protein structures were downloaded from the Protein Data Bank (PDB codes 3IL1 and 5BUU). The structures were then processed with the Schrödinger Suite 2014-3.²¹ The complexes were prepared for docking by using the Protein Preparation Wizard module available in the Maestro suite. Missing

side chains and hydrogens were added by adjusting the ionization and tautomerization states of the protein at physiological pH. Finally, the structures were refined with a restrained minimization with the OPLS2005 force field up to a final root mean square distance (RMSD) of 0.30 Å with respect to the input protein coordinates. Ligand structures were drawn with Maestro and then minimized by using the OPLS2005 force field.²² Docking was performed by using the standard precision (SP) docking protocol available in Glide with default parameters.²³ Considering that the AMPAR acts as a dimer with two allosteric ligands bound in two adjacent and symmetrically equivalent binding sites, sequential docking in 3IL1 and 5BUU structures was performed by centering the grid once on the centroid of the first crystallographic ligand and then on the centroid of the second one. The docking protocol was validated by redocking IDRA21 and BPAM-321 in their respective crystal structures.

Molecular dynamics (MD) simulations were performed starting from the docking complexes obtained as described above. Considering that docking into 3IL1 and 5BUU provided almost identical results and the two protein structures are very similar, MD simulations were run only with the complexes obtained with 3IL1. Simulations were run on the dimeric structure of the receptor with two allosteric ligands, one bound to each subunit. Simulations were performed also for the analog without the furan ring (IDRA21), for comparison.

MD simulations were carried out with the Amber 14 software package, using the ff14SB force field for the protein and the GAFF force field for the ligands. Ligands were prepared with the Antechamber module by assigning AM1-BCC atomic charges and GAFF atom types.²⁴ The system was neutralized by adding chloride ions (Cl⁻) according to the Coulomb potential grid as calculated with Leap. Afterwards, the system was solvated with a rectangular box of TIP3P water molecules placed within 10 Å distance from the solute.²⁵ Energy minimization and MD were performed with the Particle Mesh Ewald Molecular Dynamics (PMEMD) CUDA version software, employing a 12 Å cut-off for non-bonded interactions and the SHAKE algorithm and a 2 fs time step.²⁶ 3000 steps of steepest descent and conjugate gradient energy minimization were performed on water molecules and ions first, keeping the protein and the two ligands in place using harmonic constraints. Then, 1000 steps of energy minimization were conducted without constraints.

The system was heated from 0 to 300 K with 100 ps constant volume Langevin MD and a collision frequency of 2.0 ps⁻¹, keeping the protein and the ligands in place using a 5 kcal mol⁻¹ Å² harmonic constraint. Then, constraints were gradually reduced in 2 ns turning to constant pressure MD, and equilibration was performed for 0.5 ns without constraints. After equilibration, a 20 ns MD production run was performed for each complex and coordinates were collected every 100 ps. For each system, MD simulations were run in three replicates. Trajectories were analyzed with the CPPTRAJ module available in Amber.²⁷

Free energies of binding were calculated by using the parallel version of the MMPBSA.py module available in Amber.²⁸ Free energies were calculated with MM-PBSA on 200 equally spaced frames collected during the 20 ns production run. All water molecules and counterions were removed except for six (three for each subunit) water molecules that make important hydrogen bond bridges between the protein and the ligand. These water molecules (W317, W459, W485, W595, W610, W766, the numbering refers to the 3IL1 PDB crystal structure) are present in most crystal structures of the AMPA receptor in complex with ligands.

Free energies reported in Table 1 are the averages of the energies obtained in the three replicates.

3.5 Metabolic studies

The experiments were performed at t_0 (the reaction was stopped right after the addition of microsomes) and t_{60} (the reaction was stopped after 60 minutes from the addition of microsomes) following a literature known procedure.²⁹ The experiments were carried out using the test compound and a negative control (without NADPH). Each experiment at t_0 and t_{60} except for the negative control was performed in duplicate. Each Eppendorf tube contained: 432 μL of 0.1 M phosphate buffer (pH 7.4) pre-warmed at 37 $^\circ\text{C}$, 50 μL of 10 mM NADPH (in the negative control, it was replaced with phosphate buffer) and 5 μL of the test compound (10 μM solution in phosphate buffer). After 5 min incubation at 37 $^\circ\text{C}$, 13 μL of microsomes at a concentration of 20 mg protein mL^{-1} were added. The reactions at t_0 were stopped with 250 μL of ice-cold methanol, and then the mixture was vortexed well. The reactions at t_{60} were incubated at 37 $^\circ\text{C}$ for 60 minutes, then stopped with 250 μL of ice-cold methanol and vortexed well. The samples were centrifuged at 10 000g for 5 min at 4 $^\circ\text{C}$. The supernatants were placed in HPLC vials and analysed with the suitable LC-MS/MS method. The pellets were stored in the freezer until all the samples were analysed.³⁰

3.6 LC-MS/MS method for the determination of *R*-4 and *S*-4

The LC-MS/MS method developed was employed for both the determination of the enantiomeric excess after semipreparative enantioseparation of *R*-4 and *S*-4 and their quantification in the microsomal media. The samples were injected on the Chiralcel® OD-RH column (150 \times 4.6 mm I. D., 5 μm ; Chiral Technologies Europe, Bd Gonthier d'Andernach, Illkirch-Cedex, France); the mobile phase was composed of water with 0.1% formic acid and ACN (50 : 50, v/v), pumped in isocratic mode at a flow rate of 0.5 mL min^{-1} . An Agilent 6410 triple quadrupole-mass spectrometer with an electrospray ionization source operating in positive mode was used to evaluate the enantiomeric excess and to analyse the microsomal extracts. The analyses were followed in selected reaction monitoring (SRM) mode to improve the sensitivity: 299 \rightarrow 218 (154) was the transition selected for both *R*-4 and *S*-4. The chromatograms were integrated using Agilent Mass Hunter software (B.06.00).

4. Conclusions

In conclusion, the isolation of the single enantiomers of 4 by semipreparative chiral chromatography has been reported. Electrophysiological results, which showed unexpectedly a higher *in vitro* AMPA PAM activity for *R*-4 compared to *S*-4, are in contrast to those reported for the lead compound IDRA21, for which the *S* form is the eutomer. Docking studies and molecular dynamics simulations were employed to understand the different stereoselectivities. The data obtained suggested a relevant role of an H-bond with Pro494 in the stereodiscrimination process. Bulkier molecules might interact more favourably with an *R* configuration in order to fit into the binding pocket. The binding of the *R* isomer leads to the loss of the interaction with Pro494. However, this deficit seems to be overcome by the contribution of van der Waals interactions and/or by H-bonding with water molecules. Binding free energy predictions suggested that in the case of compound 4 gas-phase interaction energy and desolvation energy cooperate to favour the *R* enantiomer. The metabolism of the single enantiomers of compound 4 was also investigated. The protocol outcome underlined a stereoselective hepatic metabolism for the *S* enantiomer. The results obtained in this work highlight that not only the stereochemistry of the chiral centre determines the stereoselective binding with the target receptor, but also structural chemical elements far from the stereogenic centre are responsible for the stereodiscrimination process and consequently for the biological activity.

References

- (a) R. Dingleline, K. Borges, D. Bowie and S. Traynelis, *Pharmacol. Rev.*, 1999, **51**, 7–61; (b) M. L. Mayer and N. Armstrong, Structure and function of glutamate receptor ion channels, *Annu. Rev. Physiol.*, 2004, **66**, 161–181.
- G. L. Collingridge and J. C. Watkins, *The NMDA Receptor*, Oxford University Press, Oxford, 1994.
- J. N. C. Kew and J. A. Kemp, *Psychopharmacology*, 2005, **179**, 4–29.
- U. Staubli, G. Rogers and G. Lynch, *Proc. Natl. Acad. Sci. U. S. A.*, 1994, **91**, 777–781.
- U. Staubli, Y. Perez, F. B. Xu, G. Rogers, M. Ingvar, S. Stone-Elander and G. Lynch, *Proc. Natl. Acad. Sci. U. S. A.*, 1994, **91**, 11158–11162.
- (a) P. Francotte, P. de Tullio and P. Fraikin, *Recent Pat. CNS Drug Discovery*, 2006, **1**, 239–246; (b) S. E. Ward and M. Harries, *Curr. Med. Chem.*, 2010, **17**, 3503–3513; (c) B. Pirotte, P. Francotte, E. Goffin and P. De Tullio, *Expert Opin. Ther. Pat.*, 2013, **23**, 615–628; (d) S. E. Ward, L. E. Pennicott and P. Beswick, *Future Med. Chem.*, 2015, **7**, 473–491; (e) B. Cox and M. Gosling, *Ion Channel Drug Discovery*, RSC Drug Discovery Series, 2015; (f) K. M. Partin, *Curr. Opin. Pharmacol.*, 2015, **20**, 46–53.
- (a) M. J. O'Neill, D. Bleakman, D. M. Zimmerman and E. S. Nisenbaum, *Curr. Drug Targets: CNS Neurol. Disord.*, 2004, **3**,

- 181–194; (b) C. A. Zarate and H. K. Manji, *Exp. Neurol.*, 2008, **211**, 7–10.
- 8 D. C. Goff, L. Leahy, I. Berman, T. Posever, L. Herz, A. C. Leon, S. A. Johnson and G. Lynch, *J. Clin. Psychopharmacol.*, 2001, **21**, 484–487.
- 9 (a) G. Lynch, *Curr. Opin. Pharmacol.*, 2004, **4**, 4–11; (b) M. J. O'Neill and S. Dix, *IDrugs*, 2007, **10**, 185–192.
- 10 L. A. Adler, R. A. Kroon, M. Stein, M. Shahid, F. I. Tarazi, A. Szegedi, J. Schipper and P. Cazorla, *Biol. Psychiatry*, 2012, **72**, 971–977.
- 11 K. Hashimoto, *Brain Res. Rev.*, 2009, **61**, 105–123.
- 12 B. Pirotte, P. Francotte and E. Goffin, *Curr. Med. Chem.*, 2010, **17**, 3575–3582.
- 13 (a) A. I. Sobolevsky, M. P. Rosconi and E. Gouaux, *Nature*, 2009, **462**, 745–756; (b) Y. Sun, R. Olson, M. Horning, N. Armstrong, M. Mayer and E. Gouaux, *Nature*, 2002, **417**, 245–253; (c) R. Jin, S. Clark, A. M. Weeks, J. T. Dudman, E. Gouaux and K. M. Partin, *J. Neurosci.*, 2005, **25**, 9027–9036.
- 14 C. P. Ptak, A. H. Ahmed and R. E. Oswald, *Biochemistry*, 2009, **48**, 8594–8602.
- 15 U. M. Battisti, K. Jozwiak, G. Cannazza, G. Puia, G. Stocca, D. Braghiroli, C. Parenti, L. Brasili, M. M. Carrozzo, C. Citti and L. Troisi, *ACS Med. Chem. Lett.*, 2012, **3**, 25–29.
- 16 M. M. Carrozzo, U. M. Battisti, G. Cannazza, G. Puia, F. Ravazzini, A. Falchicchio, S. Perrone, C. Citti, K. Jozwiak, D. Braghiroli, C. Parenti and L. Troisi, *Bioorg. Med. Chem.*, 2014, **22**, 4667–4676.
- 17 A. P. Larsen, P. Francotte, K. Frydenvang, D. Tapken, E. Goffin, P. Fraikin, D.-H. Caignard, P. Lestage, L. Danober, B. Pirotte and J. S. Kastrop, *ACS Chem. Neurosci.*, 2016, **7**, 378–390.
- 18 K. Bernard, L. Danober, J.-Y. Thomas, C. Lebrum, C. Munoz, A. Cordi, P. Desos, P. Lestage and P. Morain, *CNS Neurosci. Ther.*, 2010, **16**, e193–e212.
- 19 (a) G. Cannazza, U. M. Battisti, M. M. Carrozzo, A. S. Cazzato, D. Braghiroli, C. Parenti and L. Troisi, *J. Chromatogr. A*, 2014, **1363**, 216–225; (b) G. Cannazza, M. M. Carrozzo, U. Battisti, D. Braghiroli and C. Parenti, *J. Chromatogr. A*, 2009, **1216**, 5655–5659; (c) G. Cannazza, U. Battisti, M. M. Carrozzo, L. Brasili, D. Braghiroli and C. Parenti, *Chirality*, 2011, **23**, 851–859; (d) G. Cannazza, M. M. Carrozzo, U. Battisti, D. Braghiroli, C. Parenti, A. Troisi and L. Troisi, *Chirality*, 2010, **22**, 789–797; (e) M. M. Carrozzo, G. Cannazza, U. Battisti, D. Braghiroli and C. Parenti, *Chirality*, 2010, **22**, 389–397; (f) G. Cannazza, M. M. Carrozzo, D. Braghiroli and C. Parenti, *J. Chromatogr., B: Anal. Technol. Biomed. Life Sci.*, 2008, **875**, 192–199; (g) G. Cannazza, D. Braghiroli, P. Iuliani and C. Parenti, *Tetrahedron: Asymmetry*, 2006, **22**, 3158–3162.
- 20 K. Murase, P. D. Ryu and M. Randic, *Neurosci. Lett.*, 1989, **103**, 56.
- 21 Schrödinger Release 2014-3; Schrödinger Suite 2014-3 Protein Preparation Wizard; *Epik version 2.9*, Schrödinger, LLC, New York, NY, 2014; *Impact version 6.4*, Schrödinger, LLC, New York, NY, 2014; *Prime version 3.7*, Schrödinger, LLC, New York, NY, 2014.
- 22 W. L. Jorgensen, D. S. Maxwell and J. Tirado-Rives, *J. Am. Chem. Soc.*, 1996, **118**, 11225–11236.
- 23 (a) R. A. Friesner, J. L. Banks, R. B. Murphy, T. A. Halgren, J. J. Klicic, D. T. Mainz, M. P. Repasky, E. H. Knoll, D. E. Shaw, M. Shelley, J. K. Perry, P. Francis and P. S. Shenkin, *J. Med. Chem.*, 2004, **47**, 1739–1749; (b) T. A. Halgren, R. B. Murphy, R. A. Friesner, H. S. Beard, L. L. Frye, W. T. Pollard and J. L. Banks, *J. Med. Chem.*, 2004, **47**, 1750–1759; (c) *Small-Molecule Drug Discovery Suite 2014-4: Glide, version 6.5*, Schrödinger, LLC, New York, NY, 2014.
- 24 (a) D. A. Case, V. Babin, J. T. Berryman, R. M. Betz, Q. Cai, D. S. Cerutti, T. E. Cheatham III, T. A. Darden, R. E. Duke, H. Gohlke, A. W. Goetz, S. Gusarov, N. Homeyer, P. Janowski, J. Kaus, I. Kolossváry, A. Kovalenko, T. S. Lee, S. LeGrand, T. Luchko, R. Luo, B. Madej, K. M. Merz, F. Paesani, D. R. Roe, A. Roitberg, C. Sagui, R. Salomon-Ferrer, G. Seabra, C. L. Simmerling, W. Smith, J. Swails, R. C. Walker, J. Wang, R. M. Wolf, X. Wu and P. A. Kollman, *AMBER 14*, University of California, San Francisco, 2014; (b) V. Hornak, R. Abel, A. Okur, B. Strockbine, A. Roitberg and C. Simmerling, *Proteins*, 2006, **65**, 712–725; (c) J. Wang, R. M. Wolf, J. W. Caldwell, P. A. Kollman and D. A. Case, *J. Comput. Chem.*, 2004, **25**, 1157–1174; (d) B. Wang and K. M. J. Merz, *J. Chem. Theory Comput.*, 2006, **2**, 209–215; (e) A. Jakalian, B. L. Bush, D. B. Jack and C. I. Bayly, *J. Comput. Chem.*, 2000, **21**, 132–146; (f) A. Jakalian, D. B. Jack and C. I. Bayly, *J. Comput. Chem.*, 2002, **23**, 1623–1641.
- 25 W. L. Jorgensen, J. Chandrasekhar, J. D. Madura, R. W. Impey and M. L. Klein, *J. Chem. Phys.*, 1983, **79**, 926–935.
- 26 (a) A. W. Goetz, M. J. Williamson, D. Xu, D. Poole, S. L. Grand and R. C. Walker, *J. Chem. Theory Comput.*, 2012, **8**, 1542–1555; (b) R. Salomon-Ferrer, A. W. Goetz, D. Poole, S. L. Grand and R. C. Walker, *J. Chem. Theory Comput.*, 2013, **9**, 3878–3888; (c) R. C. Walker, *Comput. Phys. Commun.*, 2013, **184**, 374–380.
- 27 D. R. Roe and T. E. Cheatham, *J. Chem. Theory Comput.*, 2013, **9**, 3084–3095.
- 28 B. R. Miller III, T. D. McGee Jr., J. M. Swails, N. Homeyer, H. Gohlke and A. E. Roitberg, *J. Chem. Theory Comput.*, 2012, **8**, 3314–3321.
- 29 J. R. Hill, in *Current Protocols in Pharmacology*, John Wiley & Sons, Inc., 2003, ch. 7.8, vol. 23, pp. 1–11.
- 30 C. Citti, U. M. Battisti, G. Cannazza, K. Jozwiak, N. Stasiak, G. Puja, F. Ravazzini, G. Ciccarella, D. Braghiroli, C. Parenti, L. Troisi and M. Zoli, *ACS Chem. Neurosci.*, 2016, **7**, 149–160.
- 31 M. D. Parenti and G. Rastelli, *Biotechnol. Adv.*, 2012, **30**, 244–250.
- 32 U. M. Battisti, C. Citti, M. Larini, G. Ciccarella, N. Stasiak, L. Troisi, D. Braghiroli, C. Parenti, M. Zoli and G. Cannazza, *J. Chromatogr. A*, 2016, **1443**, 152–161.